# *The rational design of nitric oxide selectivity in single-walled carbon nanotube near infrared fluorescence sensors for biological detection*

# The Rational Design of Nitric Oxide Selectivity in Single-Walled Carbon Nanotube Near Infrared Fluorescence Sensors for Biological Detection

Jong-Ho Kim[1], Daniel A. Heller[1], Hong Jin[1], Paul W. Barone[1], Changsik Song[1], Jingqing Zhang[1], Laura J. Trudel[2], Gerald N. Wogan[3], Steven R. Tannenbaum[3], and Michael S. Strano[1,*]

[1] Department of Chemical Engineering, Massachusetts Institute of Technology, Cambridge, MA 02139, USA
[2] Department of Biological Engineering, Massachusetts Institute of Technology, Cambridge, MA 02139, USA
[3] Department of Biological Engineering and Chemistry, Massachusetts Institute of Technology, Cambridge, MA 02139, USA

[*] To whom correspondence should be addressed. Email: strano@mit.edu

## Abstract

A major challenge in the synthesis of nanotube or nanowire sensors is imparting selective analyte binding through means other than covalent linkages which compromise electronic and optical properties. We synthesize a 3,4-diaminophenyl-functionalized dextran (DAP-dex) wrapping for single-walled carbon nanotubes (SWNT) that imparts rapid and selective fluorescence detection of NO, a messenger for biological signaling. The near infrared (nIR) fluorescence of $SWNT_{DAP\text{-}dex}$ is immediately and directly bleached by NO, but not by other reactive nitrogen and oxygen species. This bleaching is reversible and shown to be caused by electron transfer from the top of the valence band of SWNT to the lowest unoccupied molecular orbital (LUMO) of NO. The resulting optical sensor is capable of real-time and spatially resolved detection of NO produced by stimulating NO synthase (iNOS) in macrophage cells. We also demonstrate the potential of the optical sensor for *in-vivo* detection of NO in a mouse model.

Since the discovery that nitric oxide (NO) is identical with endothelium-derived relaxing factor (EDRF) biosynthesized in living organisms, NO has been well known as a ubiquitous messenger in the cardiovascular and nervous systems and is employed in the human immune response[1-5]. Although NO is a relatively stable free radical, it is difficult to detect directly and in real-time *in vivo*, because of its large diffusivity and high reactivity with other radicals and metal-containing proteins in biological systems[6]. The NO radical is currently detected using several methods such as visible fluorescent probes[7-10], chemiluminescence[11], x-ray photoelectron[12] and electron paramagnetic resonance (EPR)[6] spectroscopy. In particular, a series of diaminofluoreceins[7,8] and metal-fluorophore complexes[9,10] have been widely applied to cellular NO detection. However, each method proposed to date has significant limitations. Widely used diaminofluoresceins only indirectly detect NO through its oxidation products. Other limitations include photobleaching and lack of optical penetration through biological tissues for metal-fluorophore complexes. Therefore, the design of more robust schemes for biological NO detection is still an active area of research, particularly for *in vivo* applications.

Single-walled carbon nanotubes (SWNT) are single graphene sheets in a cylindrical geometry creating quantum confinement of electrons and excitons in a single dimension. Our laboratory has pioneered the development of SWNT as fluorescence sensors for biological applications including glucose[13-15], DNA[16], and divalent ions[17,18]. Recently, semiconducting SWNT exhibiting nIR photoluminescence (PL)[19,20] have been widely applied to sensing and imaging biological molecules[21-29], because its PL properties can easily be modulated in response to adsorption of small molecules such as electron-withdrawing or donating groups and organic charge-transfer dyes[13,25,30] and a change in the dielectric environment surrounding SWNT[17,31,32]. In addition, the electron donating groups such as amines improve the electron density and mobility in SWNT via donation of their lone pair electrons[33,34]. The

nIR fluorescence of SWNT has also been shown to be resistant to irreversible photobleaching with little or no threshold reported to date[21] and can penetrate more deeply into tissues than visible ones without overlapping autofluorescence from biological substrates. Due to these advantages, in this work we explore whether SWNT can act as effective sensing platforms for real-time, direct and selective detection of NO *in vitro* or *in vivo*.

A central challenge to designing selective sensors for SWNT is the engineering of selective analyte binding. Because covalent attachment of recognition groups to the SWNT surface disrupts radiative exciton recombination, other methods need to be developed[35]. For a sensor that must operate in solution, cell culture or *in-vivo*, colloidal stability is a primary issue, eliminating the viability of many non-covalent schemes proposed for electronic sensors[36]. An understanding of how to impart small molecule selectivity, maintain colloidal stability and fluorescent emission is a goal, central to enabling this application.

Herein, we describe a 3,4-diaminophenyl-functionalized dextran (DAP-dex, **5**) wrapping for SWNT that imparts rapid and selective fluorescence detection of NO in the near infrared (nIR) via donating the lone pair electrons in amines conferring more electron density and mobility in SWNT. The $SWNT_{DAP\text{-}dex}$ hybrid functions as a transition bleaching based assay for NO and has high selectivity over other reactive nitrogen and oxygen species. We show that NO binding is non-covalent and the $SWNT_{DAP\text{-}dex}$ sensor is able to reversibly detect NO via the fluorescence bleaching. Spectral evidence supports a mechanism of electron transfer from the top of the valence band of SWNT to the lowest unoccupied molecular orbital (LUMO) of the NO radical. The $SWNT_{DAP\text{-}dex}$ sensor is capable of real-time and spatially resolved detection of NO inside of living cells at the nanomolar concentration level. We demonstrate that NO produced by stimulating NO synthase (iNOS) in Raw 264.7 macrophage cells is detected in real time using the fluorescence bleaching of $SWNT_{DAP\text{-}dex}$. We also show the potential of the SWNT sensor for *in-vivo* detection of NO using any

platform by injection of the sensor complexes into a mouse animal model.

## RESULTS

### Preparation of $SWNT_{DAP\text{-}dex}$

In order to individually suspend SWNT in water and render higher selectivity and sensitivity for NO, DAP-dex (**5**) was synthesized as shown in Figure 1. Our hypothesis was that lone pair electrons on the amine moieties themselves n-dope the nanotube, making it electron-rich for direct charge transfer to NO. First, 3,4-diaminobenzoic acid (DABA, **1**) is protected with *tert*-butyloxycarbonyl (Boc) group in 40% yield[37]. 1,4-Diaminobutane is then coupled to carboxylic acid of Boc-protected DABA (Boc-DABA, **2**) in dichloromethane (DCM) for 2 h at 25$^{o}$C to give the desired product, aminobutylated Boc-DABA (Boc-DABA-$NH_2$, **3**) in 70% yield. Dextran (9-11 kDa) is carboxymethylated using chloroacetic acid in NaOH aqueous solution for 1.5 h at 60$^{o}$C[38]. According to the results of acidimetric titration and mass increase, 24 wt% of carboxylic acid (4.19 mmol-carboxylic acid/g) is introduced onto dextran (CM-dex, **4**). Boc-DABA-$NH_2$ (**3**) is coupled to carboxylic acid of dextran in water for 8 h at 25$^{o}$C, and then the Boc-protecting group is removed using phosphoric acid for 20 h at 25$^{o}$C[39] to give 3,4-diaminophenyl-functionalized dextran (DAP-dex, **5**). The absorption feature of the DAP group in DAP-dex (**5**) is observed at 260 nm in UV-vis spectra (**Fig. S1**). In addition, the amount of substituted DAP group is determined by measuring the absorbance at 260 nm after creating the calibration curve. According to UV-vis analysis, an 11 wt% of the DAP group is introduced onto CM-dex (**4**). DAP-dex (**5**) was also analyzed by FT-IR spectroscopy. Two specific bands at 1650 and 1530 $cm^{-1}$ are also observed in FT-IR spectra of DAP-dex (**5**), corresponding to the (C=O) stretching band and the (-NH) bending vibration bend, respectively (**Fig. S2**). The DAP-dex (**5**) is very soluble in water, which indicates the amount

of substituent does not diminish the solubility of the original dextran in water. For all detection experiments, DAP-dex (**5**) with a diaminophenyl content of 11 wt% was used.

To resuspend SWNT with DAP-dex (**5**), dialysis of 0.3 wt% DAP-dex and a sodium cholate (SC) suspended SWNT mixture ($SWNT_{SC}$, 12 μg/mL) against phosphate-buffered saline (PBS, 50 mM, pH 7.4) was then carried out for 24 h at 25°C[13,16], which results in removal of sodium cholate and DAP-dex suspended SWNT. As shown in AFM and optical images (**Fig. S3**), dialysis of $SWNT_{SC}$ without DAP-dex (**5**) causes SWNT aggregation, but SWNT with DAP-dex are well suspended. Approximately, 90% of the initial $SWNT_{SC}$ is shown to be resuspended with DAP-dex (**5**) based on the UV-vis-nIR absorption analysis. The fluorescence and absorption spectra (**Fig. 2a**) show that a red shift (~18 nm or 14.5 meV) occurs for the $SWNT_{DAP\text{-}dex}$ hybrid when SC is replaced with DAP-dex, which is similar with the shift that was observed in DNA-SWNT[16]. The normalized fluorescence intensity of $SWNT_{DAP\text{-}dex}$ decreases as compared to SC suspended SWNT, although the absorption intensities are similar to each other (**Fig. 2a, inset**). This behavior observed in $SWNT_{DAP\text{-}dex}$ is consistent with a mechanism of photo-induced excited-state electron transfer from the nanotube conduction band to the lowest unoccupied molecular orbital (LUMO) of an adsorbing molecule, which has been suggested before[25]. In addition, the reduction potential of the DAP group measured by cyclic voltammetry is -0.15 V (versus a normal hydrogen electrode) and therefore lies within the gap between the valence and conduction bands of SWNT in this range, which apparently supports the mechanism for the initial diminution of nIR fluorescence. In spite of this initial diminution, the residual nIR fluorescence of $SWNT_{DAP\text{-}dex}$ is adequate for NO detection, as described below.

## The nIR fluorescence response of $SWNT_{DAP\text{-}dex}$ to NO

We first investigated the nIR fluorescence response of $SWNT_{DAP\text{-}dex}$ and $SWNT_{SC}$ to NO. The NO solution was prepared by bubbling pure NO gas through PBS (50 mM, pH 7.4) that was deoxidized by bubbling argon through it for 2 h before NO introduction. The concentration of NO was measured by a horseradish peroxidase assay[7,40]. Each SWNT solution (in PBS, pH 7.4, 50 mM) was also bubbled with argon for 2 h to remove dissolved oxygen prior to NO addition. As shown in Figure 2, addition of NO solution (30 μM) to a $SWNT_{DAP\text{-}dex}$ solution leads to the immediate bleaching of nIR fluorescence (**Fig. 2b**), indicating that rapid NO detection with substantial fluorescence bleaching at a physiological pH is possible on $SWNT_{DAP\text{-}dex}$ hybrid. However, this distinct transition bleaching of fluorescence was not observed in $SWNT_{SC}$ even 30 min after the same amount of NO was added into a $SWNT_{SC}$ solution (**Fig. 2c**). These results suggest that the polymer wrapping around the SWNT mediates the NO detection by nIR fluorescence bleaching.

Therefore, we further investigated the effect of SWNT-wrapping molecules on NO detection in terms of selectivity and transition bleaching rate. We synthesized phenoxy-modified carboxymethylated-dextran (PhO-dex, **7**) that does not have amine and amide groups (**Fig. S4**), and then SWNT was resuspended with PhO-dex (**7**) via dialysis[15]. Then, we examined the fluorescence response of $SWNT_{DAP\text{-}dex}$, $SWNT_{PhO\text{-}dex}$ and $SWNT_{SC}$ for NO. As shown in Figure 3, nIR fluorescence of $SWNT_{DAP\text{-}dex}$ is selectively bleached by NO over other many other reactive nitrogen and oxygen species present in typical biological systems, including $NO_2^-$, $NO_3^-$, $ONO_2^-$, HNO, $OCl^-$, hydroxyl radical and $H_2O_2$ (**Fig. 3a**). These results indicate that $SWNT_{DAP\text{-}dex}$ may allow for NO detection *in vitro* or *in vivo*.

There is a smaller, less selective and slower response from SWNT suspended with PhO-dex ($SWNT_{PhO\text{-}dex}$), but little selectivity for NO is observed with $SWNT_{SC}$. The effect of wrapping functionalities on NO detection is more obviously observed in the transition

bleaching rates of nIR fluorescence as shown in Figure 3b and 3c. It is found that the fluorescence of $SWNT_{DAP\text{-}dex}$ is bleached by NO significantly faster than one from $SWNT_{PhO\text{-}dex}$ and $SWNT_{SC}$. The bleaching rate of $SWNT_{DAP\text{-}dex}$ ($k = 0.856\ s^{-1}$) is almost 5-fold faster than the rates of $SWNT_{PhO\text{-}dex}$ ($k = 0.217\ s^{-1}$) and $SWNT_{SC}$ ($k = 0.204\ s^{-1}$). In addition, the fluorescence of small-bandgap SWNT decays faster than large-bandgap species (**Fig. 3c**), because the difference in the gap between the valence band and LUMO of NO is greater for small-bandgap SWNTs than for large-bandgap species. The smallest concentration of NO detected in this work using $SWNT_{DAP\text{-}dex}$ is 100 nM (**Fig. 3d**). However, based on a calibration curve from Figure 3d, the concentration at 3 times the noise value for a typical experiment with *S/N* = 7 is 70 nM of NO. Therefore, we estimate this value as the current detection limit. Compared to the metal-fluorescein probe (5 nM)[9] that is irreversible for NO detection, the detection limit of $SWNT_{DAP\text{-}dex}$ is 12 times higher. Further optimization may be possible by varying the number of the diamino groups per length.

We analyzed in detail $SWNT_{DAP\text{-}dex}$ at saturation (i.e. nIR fluorescence completely bleached by NO) in order to elucidate the bleaching mechanism. As shown in Figure 4, visible and nIR absorption features of SWNT change after addition of NO. In particular, the first van Hove transitions almost disappear (**Fig. 4a**). The selectivity for small-bandgap nanotubes identifies this as a transition photobleaching mechanism as similarly seen for glucose detection[13], and reactions of SWNT with organic charge-transfer molecule[30] or $K_2IrCl_6$[41]. The Raman spectra of $SWNT_{DAP\text{-}dex}$ after addition of NO show that the intensity of the radial breathing mode relative to the G peak decreases as expected via its loss of resonance enhancement. However, an increase in the disorder mode (D) ($1290\ cm^{-1}$) is not observed (**Fig. 4b**) indicating that the attachment is non-covalent and potentially reversible. Further evidence to clarify the bleaching mechanism by NO was obtained by a recovery experiment. As shown in Figure 4c, addition of β-nicotinamide adenine dinucleotide (NADH,

reduced) that is a reducing agent to the bleached $SWNT_{DAP\text{-}dex}$ solution results in complete recovery of nIR fluorescence, indicating that the $SWNT_{DAP\text{-}dex}$ optical sensor is theoretically reversible for NO detection. In addition, nearly complete recovery of visible/nIR absorption of $SWNT_{DAP\text{-}dex}$ is observed after addition of NADH (**Fig. S6**). Both recoveries are consistent with electron transfer from NADH to the oxidized SWNT and also support a non-covalent attachment of NO to the SWNT sidewall. Therefore, we tried to dialyze out NO adsorbed on or around SWNT to evaluate the reversible detection. As shown in Figure 4d, the bleached fluorescence is restored after simply removing NO from SWNT via dialysis, indicating NO detection is reversible. The restoration occurs at the diffusion limit through the dialysis membrane, and it is therefore not possible to estimate the desorption rate constant from this experiment. Molecules of comparable size were found to have desorption rate constants between 600 and 1130 $\mu s^{-1}$ for collagen-wrapped SWNT[42], suggesting that the NO response is rapid enough for dynamic measurements. All of these results agree with the mechanism asserted above where electron transfer from the top of the nanotube valence band to LUMO of NO causes reversible transition bleaching and nIR fluorescence attenuation.

## Biological NO detection on $SWNT_{DAP\text{-}dex}$

Of particular merit is the ability to temporally and spatially determine the production of NO in complex biological systems as a means to study signaling pathways. First, we evaluated the capability of the $SWNT_{DAP\text{-}dex}$ optical sensor for real-time and spatially resolved detection of NO inside cells. Raw 264.7 murine macrophage cells were incubated with $SWNT_{DAP\text{-}dex}$ (1 μg/mL) for 12 h at 37$^{o}$C, and then washed with PBS several times. Internalization of SWNT into the cells has been well studied before[22]. As shown in Figure 5, macrophage cells incorporating $SWNT_{DAP\text{-}dex}$ inside show bright and photostable nIR fluorescence (**Fig. 5a**,

control). After this nIR fluorescence generated from the macrophage cells was monitored in real time for 330 sec, and the NO solution (5 μM, PBS) was added in the macrophage cells. The fluorescence images of macrophage cells show a decrease of fluorescence intensity upon addition of NO, and almost complete bleaching is observed 30 sec after NO treatment (**Fig. 5a**), which demonstrates that $SWNT_{DAP\text{-}dex}$ can detect NO inside the cells in real time. Despite the fact that is the sensor is based on bleaching (or "turn-off"), the photostability and small diffusion constant of SWNT enable a further analysis that is not possible with the previous organic fluorescence probes. We normalized each pixel by its corresponding intensity at the start of the experiment. As shown in Figure 5a (Imaging of NO), the result is a spatial dependence on the quenching that reflects real time gradients in NO concentration within the cell. Note that some regions clearly quench before others, and at different rates. Recent work highlights that small molecule still encounter barriers to diffusion due to the increased viscosity of dense lipid compared to the cytoplasm[43]. Hence, gradients at the cellular level are anticipated. In addition, the $SWNT_{DAP\text{-}dex}$ optical sensor enables us to quantitatively track the real-time nIR fluorescence inside the cells, as shown in Figure 5b. The nIR fluorescence intensity of $SWNT_{DAP\text{-}dex}$ inside the cells suddenly decreases upon addition of NO solution (**Fig. 5b**) with a detection limit of approximately 200 nM of NO inside the cells (**Fig. S7**). In a control experiment, Raw 264.7 macrophage cells incorporating $SWNT_{DAP\text{-}dex}$ inside were monitored in the absence of NO for 10 min (**Fig 5a**, **control**). Bright nIR fluorescence of $SWNT_{DAP\text{-}dex}$ inside the macrophage cells is still observed without photobleaching during laser irradiation for 10 min in the fluorescence images, and this is more clearly demonstrated in quantitative tracking of fluorescence intensity (**Fig. 5b**, control), indicating that the fluorescence bleaching is caused by NO production in the macrophage cells. We next evaluated the ability of $SWNT_{DAP\text{-}dex}$ to spatially detect NO inside macrophage cells by measuring the fluorescence in each cell or in the different region of a single cell. The

degree of fluorescence bleaching by NO clearly varies among the cells (**Fig. S8, b**). The overall fluorescence from three individual cells is bleached approximately 40, 28 and 20% after addition of NO. Moreover, differences in fluorescence bleaching in different regions of the same cell can be distinguished (F**ig. S8, c**). Quantitatively, the region (x,y = 63,139) of the cell denoted with 2 (**Fig. S8, a**) is bleached by 30%, while another part (x,y =137,137) of the same cell is bleached 65%. There is no correlation with SWNT concentration (PL intensity) and we conclude that the sensors are able to resolve gradients in NO concentration present in different compartments of the same cell.

In macrophage cells, it is well known that NO is produced by inducible NO synthase (iNOS)[3,44,45]. We investigated the detection of time-dependent NO production by Raw 264.7 murine macrophage cells stimulated with lipopolysaccharide (LPS) and interferon-γ (IFN-γ) using $SWNT_{DAP\text{-}dex}$ optical sensor. After macrophage cells were incubated with $SWNT_{DAP\text{-}dex}$ (1 μg/mL) for 12 h at 37$^{o}$C and washed with PBS, they were treated with LPS (20 ng/mL) and IFN-γ (20 U/mL). After 6 h incubation, the nIR fluorescence response was monitored at 2 h intervals. As shown in Figure 5c and 5d, the average fluorescence of each cell successively and slowly decreases over 12 h post activation. The fluorescence bleaching response for Raw 264.7 cells pretreated with $N^{G}$-methyl-L-arginine (L-NMA, 2 mM), a known inhibitor of iNOS that attenuates NO production, becomes weaker upon LPS and IFN-γ addition. We note that the fluorescence bleaching is not observed for Raw 264.7 cells incorporating $SWNT_{DAP\text{-}dex}$ without LPS and IFN-γ stimulation. The average fluorescence intensity is almost constant for the 12 h period of the experiment in non-activated Raw 264.7 cells (**Fig. 5c and 5d**). These results clearly demonstrate that $SWNT_{DAP\text{-}dex}$ allows the detection of NO produced by iNOS in Raw 264.7 macrophage cells.

Finally, we demonstrate the potential for *in vivo* detection of NO using $SWNT_{DAP\text{-}dex}$ (**Fig.**

**5e**). A dialysis membrane loaded with a $SWNT_{DAP\text{-}dex}$ solution was inserted into a slit in the abdomen of a $CO_2$ asphyxiated mouse. Following imaging, a NO solution (60 μM) was injected in the region of the slit and the fluorescence response was monitored in real-time. As shown in Figure 5e, the nIR fluorescence is able to penetrate through tissue and with high signal to noise. After 10 min following NO injection, the fluorescence of $SWNT_{DAP\text{-}dex}$ is completely bleached. The experiment demonstrates that the major barriers to optical detection of NO *in vivo*, namely tissue penetration, scattering and autofluorescence, can be overcome using this platform, however, further work is warranted.

## Cytotoxicity of $SWNT_{DAP\text{-}dex}$ on Raw 264.7 cells

In order to evaluate the cytotoxicity of $SWNT_{DAP\text{-}dex}$, the LIVE/DEAD viability and cytotoxicity assay that provides simultaneous determination of live and dead cells with two probes[46] was carried out on Raw 264.7 cells after 12 h incubation with $SWNT_{DAP\text{-}dex}$ (1 and 2 μg/mL). According to the results of the test (**Fig. S9**), the survival and death rates of macrophage cells are 100 ± 19% and 2.4 ± 19% respectively, within the margins of error of the control samples. This indicates that $SWNT_{DAP\text{-}dex}$ is clearly not cytotoxic at all concentrations tested in this work.

In addition to cytotoxicity, we were also interested in whether $SWNT_{DAP\text{-}dex}$ would induce an activation response in Raw 264.7 cells without LPS and IFN-γ. Such a response would prevent the use of the sensor *in vitro* and *in vivo* in this capacity, since the probe itself would stimulate NO from the host immune system. We utilized the Griess assay to independently assess activation of cells exposed to $SWNT_{DAP\text{-}dex}$ with none detected (**Fig. S10**). The lack of cytotoxicity and immunogenicity is promising for practical applications of the sensor.

## DISCUSSION

In this work, we have demonstrated the first NO sensor based on SWNT that produces photostable and tissue penetrative nIR fluorescence for biological detection at neutral pH in living cells and animals.

The nIR fluorescence of $SWNT_{DAP\text{-}dex}$ is immediately and selectively bleached by the NO radical over other reactive nitrogen and oxygen species such as $NO_2^-$, $NO_3^-$, HNO, $ONOO^-$, $OCl^-$, hydroxyl radical and $H_2O_2$. Other oxidative species such as β-nicotinamide adenine dinucleotide ($NAD^+$) and ferric iron ($Fe^{3+}$) that exist in physiological systems could interfere with selectivity for NO detection. However, these species at the same concentration (30 μM) as NO used in this work do not bleach the fluorescence of $SWNT_{DAP\text{-}dex}$ appreciably (**Fig. S5**). Therefore, potential interference from oxidative agents can be excluded. Moreover, the transition bleaching rate of $SWNT_{DAP\text{-}dex}$ is at least 5-fold faster than the rates of control $SWNT_{PhO\text{-}dex}$ and $SWNT_{SC}$ (**Fig. 3**), which indicates that DAP-dex wrapping around SWNT is responsible for selectivity and rapid response to NO. Both are critical for real-time and immediate detection of NO that would be valuable to determine temporal distribution of NO in biological system. Apparently, the nanotube surface itself has a basal response to NO, as demonstrated in the cases of SC and PhO-dex controls. The DAP groups, then, increase the rate of NO detection and selectivity by donating lone pair electrons in the diamino groups to SWNT, conferring an increase in electron density. This charge-transfer n-type doping of SWNT increases the Fermi level and therefore the electrochemical potential from the LUMO of NO. This accelerates the electron transfer from SWNT to NO. Preferential reaction of NO via these diamine sites explains both the increase in rate and selectivity for NO for $SWNT_{DAP\text{-}dex}$. This also illustrates that fact that engineering a SWNT sensor in this manner requires suppression of any non-selective response from interfering molecules.

The emerging picture suggests how one may rationally design sensors for any analyte from SWNT. There are apparently two components to this selectivity induced by the polymer: its steric adsorption and its redox properties on the nanotube. There is currently no precise analytical tool to determine how a polymer adsorbs to create a selective gap or binding site for a molecule such as NO. In this way, the response to NO and a host of other probe molecules are the best probes of this adsorbed phase. This is the primary way in which adsorbents are characterized: via molecular penetration experiments. The dextran backbone alone does not adsorb to the SWNT. The phenylation allows this adsorption. The phenyl ring would have a minimum energy configuration in the pi-stacking position, so the picture is one where these rings tether a dextran backbone to the SWNT with dextran facing solution. The addition of the diamine does two things apparently. It n-dopes the carbon nanotube, raising the Fermi-level as with the case of many other amine species. It also perturbs the structure of this polymer, altering its conformation yielding a binding site that is clearly more favorable to NO binding. The best evidence for this is simply the selectivity towards NO, which increases dramatically with diamine addition. Note that this effect is not what the diamine construct does for conventional NO sensors.

The exact nature of the NO/SWNT interaction warrants further consideration. According to the results of spectroscopic analysis and recovery experiments (**Fig. 4**), the fluorescence bleaching is caused by non-covalent adsorption of NO radical and is reversible. Previous literature suggests that carbon nanotubes can scavenge radical species via radical addition (covalent) to the sidewall of nanotubes[47,48]. However, we see no evidence of this in the Raman spectra (**Fig. 4b**). Absorption analysis and recovery experiments also support the redox mechanism caused by non-covalent adsorption via electron transfer rather than covalent radical addition. In addition, the stated bleaching mechanism of electron transfer from the top of the valence band of SWNT to LUMO of NO is thermodynamically favorable,

since the reduction potential of NO to $^{3}NO^{-}$ is +0.39 V (versus a normal hydrogen electrode)[49] and below the valence bands for most nanotube species[30].

$SWNT_{DAP\text{-}dex}$ is able to detect temporally and spatially NO in living cells with distinct bleaching of its nIR fluorescence (**Fig. 5**). This has clear utility for elucidating the biological roles of ubiquitous NO. We made a point to show the capability for real-time tracking in both living cells and strongly scattering tissues. In results so far, we see significant cell-to-cell and compartmental variation in *in-vitro* experiments (**Fig. S8**). This supports the notion that $SWNT_{DAP\text{-}dex}$ can report the spatial distribution of NO and its gradients produced in complex biological systems. This type of real-time information for spatial NO production may be useful to study the physiological and pathophysiological roles of NO in biology. Endogenous detection of NO produced by iNOS in stimulated Raw 264,7 macrophage cells (**Fig. 5c and 5d**) and the result of Griess assay (**Fig. S10**) indicate that the amount of $SWNT_{DAP\text{-}dex}$ (1 μg/mL) used for cellular NO detection does not influence the primary biological pathways for NO production. Finally, the nIR fluorescence of $SWNT_{DAP\text{-}dex}$ is capable of penetrating mouse tissue and shows potential for the *in vivo* detection of NO, a longstanding goal in the field that is difficult or impossible for diaminofluorescein and metal-fluorophore indicators. To our knowledge, $SWNT_{DAP\text{-}dex}$ is the first SWNT-based sensor capable of reversible, selective, direct and real-time detection of NO *in vitro* and potentially *in vivo*.

In summary, we have demonstrated the $SWNT_{DAP\text{-}dex}$ optical sensor for reversible NO detection *in vitro* and potentially *in vivo*. NO can be detected reversibly, directly and spatiotemporally via a nIR fluorescence bleaching of SWNT. The fluorescence bleaching is clearly mediated by NO adsorption to SWNT and ultimately caused by electron transfer from the top of the SWNT valence band to LUMO of NO. In addition, $SWNT_{DAP\text{-}dex}$ has been applied to endogenous detection of NO produced by iNOS in stimulated Raw 264.7 macrophage cells and shows its possibility for *in vivo* detection of NO in a mouse.

## METHODS

### Synthesis of DAP-functionalized dextran (DAP-dex, 5)

A 3.0 g portion of 3,4-diaminobenzoic acid (**1**, DABA, 19.71 mmol) was dissolved in 100 mL of *N*,*N*-dimethylformamide (DMF), and 7.64 g of *N*,*N*-diisopropylethylamine (DIEA, 59.13 mmol) was added into DABA/DMF solution. A 10.32 g portion of di-*tert*-butyl dicarbonate ($(Boc)_2O$, 47.30 mmol) was slowly added into the DABA mixture in an ice bath, and then the resulting solution was allowed to stir for 20 h at 25°C. In order to work up the reaction, an excess of dichloromethane (DCM) was added into the reaction mixture, and then the di-Boc-protected product (**2**, Boc-DABA) was extracted with an excess of aqueous NaOH solution (1M, 500 mL). After acidifying the aqueous solution with HCl aqueous solution (1 M), Boc-DABA was immediately extracted with an excess of ethyl acetate (EA). After evaporating EA, Boc-DABA was purified with column chromatography (hexane:EA, 2:1 v/v) in 40% yield.

In order to synthesize [5-(4-amino-butylcarbamoyl)-2-*tert*-butoxycarbonylamino-phenyl]-carbamic acid *tert*-butyl ester (**3**, Boc-DABA-$NH_2$), 1.98 mL of 1,4-diaminobutane (19.72 mmol) was dissolved in 60 mL of DCM. After dissolving 1.39 g of Boc-DABA (**2**, 3.94 mmol), 1.92 g of (benzotriazol-1-yloxy)tris(dimethylamino)phosphonium hexafluoro-phosphate (BOP, 4.34 mmol) and 0.89 mL of DIEA (5.13 mmol) in 40 mL of DCM, the mixture solution was dropwise added to 1,4-diaminobutane solution for 20 min at 25°C. The resulting mixture was allowed to stir further for 3h at 25°C. After evaporating DCM, the desired product, Boc-DABA-NH2 (**3**), was separated using column chromatography (DCM:MeOH, 5:1 v/v) in 70% yield.

To 1.0 g of carboxymethylated dextran (10 kDa, 4.19 mmol/g) dissolved in 30 mL of $H_2O$[38], 0.8 g of *N*-(3-dimethylaminopropyl)-*N*′-ethylcarbodiimide hydrochloride (EDC·HCl,

4.19 mmol) and 0.96 g of *N*-hydroxysuccinimide (NHS, 8.38 mmol) were added. After dissolving 0.89 g of Boc-DABA-$NH_2$ in DMF, this solution was added into the dextran solution. The resulting mixture was allowed to stir for 10 h at 25$^{o}$C. Then, after evaporating $H_2O$ with addition of 30 mL EtOH, the reagents were washed out with EtOH several times to get the pure product. Boc-protecting group was removed in the aqueous solution of 2.46 g $H_3PO_4$ (25.14 mmol) for 20 h at 25$^{o}$C[39]. The desired product, DAP-dex (**5**) was precipitated in an excess of EtOH. Details about the characterization of compounds are provided in **Supplementary Information** online.

**Cell culture and assay**

Raw 264.7 murine macrophage cells were grown in Dulbecco's modified Eagles' media (DMEM) containing 10% (v/v) fetal bovine serum (FBS), 100 U/mL penicillin and 100 μg/mL streptomycin at 37$^{o}$C in a humidified atmosphere of 5% $CO_2$. For detection of NO produced by iNOS in stimulated Raw 264.7 cells, $SWNT_{DAP\text{-}dex}$ (1 μg/mL) was added in macrophage cells dispersed in 2 mL DMEM, and then incubated for 12 h at 37$^{o}$C for adhesion of cell and uptake of SWNT. After washing the cells with PBS several times, LPS (20 ng/mL) and IFN-γ (20 U/mL) were added in the cells. After incubation for 6 h at 37$^{o}$C, the fluorescence response inside the cells stared to be monitored by nIR fluorescence microscope.

Other methods; Additional details such as NMR, FT-IR and UV analysis for each product, nIR fluorescence, absorption and Raman spectroscopy, the procedures for *in-vivo* experiment and cytotoxicity etc. are provided in Supplemental information.

## ACKNOWLEDGMENTS

This work was supported by a Beckman Young Investigator Award to M.S.S. and the National Science Foundation. A seed grant from the Center for Environmental Health and Science at MIT is also appreciated. J.H. Kim is grateful for a postdoctoral fellowship from the Korea Research Foundation Grant funded by the Korean Government (MOEHRD) (KRF-2007-357-D00086). We also thank W.M. Deen in department of chemical engineering at MIT for discussing NO diffusion.

## AUTHOR CONTRIBUTIONS

J.H.K. and M.S.S. conceived and designed the experiments. J.H.K. performed the experiments and analyzed the data. D.A.H., H.J., P.W.B., C.S. and J.Z. assisted in doing experiments. L.J.T., G.N.W. and S.R.T. discussed the results of biological NO detection and commented on it. J.H.K. and M.S.S. co-wrote the paper.

**Figure Captions:**

**Figure 1**. **Schematic illustration for NO detection using SWNT/polymer hybrid.** a) Synthesis of 3,4-diaminophenyl-functionalized dextran (DAP-dex, **5**). b) Preparation of SWNT/DAP-dex hybrid ($SWNT_{DAP\text{-}dex}$, **6**) via dialysis and mechanism for nIR fluorescence bleaching by NO.

**Figure 2**. **nIR fluorescence response of $SWNT_{DAP\text{-}dex}$ hybrid (6) to NO**. a) nIR fluorescence and absorption (inset) spectra of $SWNT_{DAP\text{-}dex}$ containing 11 wt% of DAP content and $SWNT_{SC}$ normalized to SWNT concentration. These results show that the fluorescence intensity decreases and a red shift (14.5 meV) occurs for $SWNT_{DAP\text{-}dex}$ hybrid when SC is replaced with DAP-dex. b) Fluorescence spectra of $SWNT_{DAP\text{-}dex}$ measured 2, 4, 6, 8 and 10 sec after addition of NO solution (30 μM), showing immediate fluorescence bleaching. c) Fluorescence spectra of $SWNT_{SC}$ measured 30 sec, 1, 10 and 30 min after addition of NO solution (30 μM), showing weak response to NO. nIR fluorescence spectra were acquired for 1 sec using 785 nm excitation (85 mW).

**Figure 3**. **Selectivity, sensitivity and bleaching rate of $SWNT_{DAP\text{-}dex}$ hybrid (6) for NO**. a) Fluorescence intensity ($I/I_o$, current intensity/initial intensity based on (10,5) SWNT) of $SWNT_{DAP\text{-}dex}$, $SWNT_{PhO\text{-}dex}$ and $SWNT_{SC}$ measured 10 min after addition of 30 μM of each analyte (NO, $NO_2^-$, $NO_3^-$, $ONO_2^-$, $NO^-$ , $OCl^-$, hydroxyl radical and $H_2O_2$) in PBS solution (pH 7.4, 50 mM). b) Fluorescence bleaching rates of $SWNT_{DAP\text{-}dex}$ ($k_{DAP\text{-}dex}$: 0.856 $s^{-1}$), $SWNT_{PhO\text{-}dex}$ ($k_{PhO\text{-}dex}$: 0.217 $s^{-1}$) and $SWNT_{SC}$ ($k_{SC}$: 0.204 $s^{-1}$) at 2.7 μM concentration of NO, showing DAP functional group significantly enhances the bleaching rate for NO. The intensity of (10,5) SWNT was measured. c) Fluorescence bleaching rates for NO as a function of emission energy for $SWNT_{DAP\text{-}dex}$ and $SWNT_{PhO\text{-}dex}$. d) Sensitivity of $SWNT_{DAP\text{-}dex}$ for NO detection based on the fluorescence bleaching of (10,5) SWNT measured 10 min after addition of each NO solution. Error bars were determined from the mean and standard deviation.

**Figure 4**. **Spectroscopic analysis for fluorescence bleaching mechanism of $SWNT_{DAP\text{-}dex}$**

**hybrid by NO**. a) Absorption spectra of $SWNT_{DAP\text{-}dex}$ after addition of 30 μM NO solution, showing the large decrease of absorbance for small bandgap SWNT. b) Raman spectra of $SWNT_{DAP\text{-}dex}$ after addition of 30 μM NO solution, showing that the intensity of RBM mode decreases (inset) and the disorder mode (1290 $cm^{-1}$) is not observed after NO addition. c) Recovered fluorescence spectra of bleached $SWNT_{DAP\text{-}dex}$ after addition of NADH (150 μM), showing complete recovery of fluorescence. d) Fluorescence intensity based on (10,5) SWNT showing that the bleached fluorescence is restored by simply removing NO (30 μM) from $SWNT_{DAP\text{-}dex}$ via dialysis. Raman and nIR fluorescence spectra were acquired for 1 sec using 785 nm excitation.

**Figure 5**. **Biological NO detection using $SWNT_{DAP\text{-}dex}$ hybrid**. a) nIR fluorescence images and direct NO mappings of Raw 264.7 cells incorporating $SWNT_{DAP\text{-}dex}$ (1 μg/mL) before and after NO addition. For control experiment, the fluorescence inside Raw 264.7 cells was monitored for 10 min without NO addition. The direct NO mappings were obtained after normalizing each pixel by its corresponding initial intensity. All fluorescence images were obtained with 1 sec acquisition using 658 nm excitation (35 mW). b) Real-time tracking of nIR fluorescence response inside Raw 264.7 cells for an extra solution of NO (5 and 0.5 μM). The fluorescence intensity was a value from an entire picture plane. c) nIR fluorescence response to NO produced by iNOS in Raw 264.7 cells stimulated with LPS (20 ng/mL) and IFN-γ (20 U/mL). As a control experiment, the nIR fluorescence image was taken 12 h after incubation of Raw 264.7 cells without stimulation. d) Average fluorescence intensity from each cell region responding to NO produced by iNOS in Raw 264.7 cells stimulated with LPS and IFN-γ. After the cells were pre-stimulated with LPS and IFN-γ for 6 h, the fluorescence intensity was measured at 2 h intervals. Besides, Raw 264.7 cells were pretreated with NMA (2 mM) for 1 h and sequentially stimulated with LPS and IFN-γ for 6 h. Error bars were determined from the mean and standard deviation. e) Optical picture showing a mouse was placed on the optical stage of nIR fluorescence spectrometer and fluorescence response to NO (60 μM) inside a mouse. A laser beam focused on the abdomen side of a mouse where the dialysis membrane loaded with the $SWNT_{DAP\text{-}dex}$ solution was inserted inside. The spectra were background subtracted and obtained with 30 sec signal acquisition at 785 nm excitation.

## References.


1. Moncada, S., Palmer, R.M.J. & Higgs, E.A. Nitric-Oxide - Physiology, Pathophysiology, and Pharmacology. *Pharmacol. Rev.*, **43**, 109-142 (1991).
2. Bredt, D.S. & Snyder, S.H. Nitric Oxide - a Physiological Messenger Molecule. *Ann. Rev. Biochem.*, **63**, 175-195 (1994).
3. Murad, F. Discovery of some of the biological effects of nitric oxide and its role in cell signaling (Nobel lecture). *Angew. Chem. Int. Edit.*, **38**, 1857-1868 (1999).
4. Furchgott, R.F. Endothelium-derived relaxing factor: Discovery, early studies, and identifcation as nitric oxide (Nobel lecture). *Angew. Chem. Int. Edit.*, **38**, 1870-1880 (1999).
5. Ignarro, L.J. Nitric oxide: A unique endogenous signaling molecule in vascular biology (Nobel lecture). *Angew. Chem. Int. Edit.*, **38**, 1882-1892 (1999).
6. Nagano, T. & Yoshimura, T. Bioimaging of nitric oxide. *Chem. Rev.*, **102**, 1235-1269 (2002).
7. Kojima, H. et al. Detection and imaging of nitric oxide with novel fluorescent indicators: Diaminofluoresceins. *Anal. Chem.*, **70**, 2446-2453 (1998).
8. Sasaki, E. et al. Highly sensitive near-infrared fluorescent probes for nitric oxide and their application to isolated organs. *J. Am. Chem. Soc.*, **127**, 3684-3685 (2005).
9. Lim, M.H., Xu, D. & Lippard, S.J. Visualization of nitric oxide in living cells by a copper-based fluorescent probe. *Nat. Chem. Biol.*, **2**, 375-380 (2006).
10. Lim, M.H. & Lippard, S.J. Metal-based turn-on fluorescent probes for sensing nitric oxide. *Accounts Chem. Res.*, **40**, 41-51 (2007).
11. Robinson, J.K., Bollinger, M.J. & Birks, J.W. Luminol/$H_2O_2$ chemiluminescence detector for the analysis of nitric oxide in exhaled breath. *Anal. Chem.*, **71**, 5131-5136 (1999).
12. Dubey, M., Bernasek, S.L. & Schwartz, J. Highly sensitive nitric oxide detection using X-ray photoelectron spectroscopy. *J. Am. Chem. Soc.*, **129**, 6980-6981 (2007).
13. Barone, P.W., Baik, S., Heller, D.A. & Strano, M.S. Near-infrared optical sensors based on single-walled carbon nanotubes. *Nat. Mater.*, **4**, 86-92 (2005).
14. Barone, P.W., Parker, R.S. & Strano, M.S. In vivo fluorescence detection of glucose using a single-walled carbon nanotube optical sensor: Design, fluorophore properties, advantages, and disadvantages. *Anal. Chem.*, **77**, 7556-7562 (2005).
15. Barone, P.W. & Strano, M.S. Reversible control of carbon nanotube aggregation for a glucose affinity sensor. *Angew. Chem. Int. Edit.*, **45**, 8138-8141 (2006).
16. Jeng, E.S., Moll, A.E., Roy, A.C., Gastala, J.B. & Strano, M.S. Detection of DNA hybridization using the near-infrared band-gap fluorescence of single-walled carbon nanotubes. *Nano Lett.*, **6**, 371-375 (2006).
17. Heller, D.A. et al. Optical detection of DNA conformational polymorphism on single-walled carbon nanotubes. *Science* **311**, 508-511 (2006).
18. Jin, H. et al. Divalent ion and thermally induced DNA conformational polymorphism on single-walled carbon nanotubes. *Macromolecules* **40**, 6731-6739 (2007).
19. Bachilo, S.M. et al. Structure-assigned optical spectra of single-walled carbon nanotubes. *Science* **298**, 2361-2366 (2002).
20. O'Connell, M. J. et al. Band gap fluorescence from individual single-walled carbon nanotubes. *Science* **297**, 593-596 (2002).
21. Heller, D.A., Baik, S., Eurell, T.E. & Strano, M.S. Single-walled carbon nanotube spectroscopy in live cells: Towards long-term labels and optical sensors. *Adv. Mater.*, **17**, 2793-2799 (2005).
22. Jin, H., Heller, D.A. & Strano, M.S. Single-particle tracking of endocytosis and exocytosis of single-walled carbon nanotubes in NIH-3T3 cells. *Nano Lett.*, **8**, 1577-1585 (2008).
23. Strano, M.S. & Jin, H. Where is it heading? Single-particle tracking of single-walled carbon nanotubes. *Acs Nano* **2**, 1749-1752 (2008).
24. Choi, J.H. et al. Multimodal biomedical imaging with asymmetric single-walled carbon nanotube/iron oxide nanoparticle complexes. *Nano Lett.*, **7**, 861-867 (2007).
25. Satishkumar, B.C. et al. Reversible fluorescence quenching in carbon nanotubes for biomolecular sensing. *Nat. Nanotechnol.*, **2**, 560-564 (2007).
26. Cognet, L. et al. Stepwise quenching of exciton fluorescence in carbon nanotubes by single-molecule

reactions. *Science* **316**, 1465-1468 (2007).
27. Cherukuri, P. et al. Mammalian pharmacokinetics of carbon nanotubes using intrinsic near-infrared fluorescence. *Proc. Natl Acad. Sci. U. S. A.,* **103**, 18882-18886 (2006).
28. Cherukuri, P., Bachilo, S.M., Litovsky, S.H. & Weisman, R.B. Near-infrared fluorescence microscopy of single-walled carbon nanotubes in phagocytic cells. *J. Am. Chem. Soc.,* **126**, 15638-15639 (2004).
29. Welsher, K., Liu, Z., Daranciang, D. & Dai, H. Selective probing and imaging of cells with single walled carbon nanotubes as near-infrared fluorescent molecules. *Nano Lett.,* **8**, 586-590 (2008).
30. O'Connell, M.J., Eibergen, E.E. & Doorn, S.K. Chiral selectivity in the charge-transfer bleaching of single-walled carbon-nanotube spectra. *Nat. Mater.,* **4**, 412-418 (2005).
31. Walsh, A.G. et al. Screening of excitons in single, suspended carbon nanotubes. *Nano Lett.,* **7**, 1485-1488 (2007).
32. Choi, J.H. & Strano, M.S. Solvatochromism in single-walled carbon nanotubes. *Appl. Phys. Lett.,* **90**, 223114 (2007).
33. Klinke, C., Chen, J., Afzali, A. & Avouris, P. Charge transfer induced polarity switching in carbon nanotube transistors. *Nano Lett.,* **5**, 555-558 (2005).
34. Shim, M., Javey, A., Kam, N.W.S. & Dai, H. Polymer functionalization for air-stable n-type carbon nanotube field-effect transistors. *J. Am. Chem. Soc.,* **123**, 11512-11513 (2001).
35. Usrey, M.L., Lippmann, E.S. & Strano, M.S. Evidence for a two-step mechanism in electronically selective single-walled carbon nanotube reactions. *J. Am. Chem. Soc.,* **127**, 16129-16135 (2005).
36. Cui, Y., Wei, Q.Q., Park, H.K. & Lieber, C.M. Nanowire nanosensors for highly sensitive and selective detection of biological and chemical species. *Science* **293**, 1289-1292 (2001).
37. Eisenhut, M. et al. Melanoma uptake of Tc-99m complexes containing the N-(2-diethylaminoethyl) benzamide structural element. *J. Med. Chem.,* **45**, 5802-5805 (2002).
38. Mauzac, M. & Jozefonvicz, J. Anticoagulant Activity of Dextran Derivatives .1. Synthesis and Characterization. *Biomaterials* **5**, 301-304 (1984).
39. Li, B. et al. Aqueous phosphoric acid as a mild reagent for deprotection of tert-butyl carbamates, esters, and ethers. *J. Org. Chem.,* **71**, 9045-9050 (2006).
40. Kikuchi, K., Nagano, T. & Hirobe, M. Novel detection method of nitric oxide using horseradish peroxidase. *Biol. Pharm. Bull.,* **19**, 649-651 (1996).
41. Zheng, M. & Diner, B.A. Solution redox chemistry of carbon nanotubes. *J. Am. Chem. Soc.,* **126**, 15490-15494 (2004).
42. Jin, H., Heller, D.A., Kim, J.H. & Strano, M.S. Stochastic Analysis of Stepwise Fluorescence Quenching Reactions on Single-Walled Carbon Nanotubes: Single Molecule Sensors. *Nano Lett.,* **8**, 4299-4304 (2008).
43. Kuimova, M.K., Yahioglu, G. & Ogilby, P.R. Singlet Oxygen in a Cell: Spatially Dependent Lifetimes and Quenching Rate Constants. *J. Am. Chem. Soc.,* **131**, 332-340 (2009).
44. Ricciardolo, F.L. M., Sterk, P.J., Gaston, B. & Folkerts, G. Nitric oxide in health and disease of the respiratory system. *Physiol. Rev.,* **84**, 731-765 (2004).
45. Zhuang, J.C. & Wogan, G.N. Growth and viability of macrophages continuously stimulated to produce nitric oxide. *Proc. Natl. Acad. Sci. U. S. A.,* **94**, 11875-11880 (1997).
46. Pike, C.J., Overman, M.J. & Cotman, C.W. Amino-Terminal Deletions Enhance Aggregation of Beta-Amyloid Peptides in-Vitro. *J. Biol. Chem.,* **270**, 23895-23898 (1995).
47. Fenoglio, I. et al. Reactivity of carbon nanotubes: Free radical generation or scavenging activity?. *Free Radic. Biol. Med.,* **40**, 1227-1233 (2006).
48. Galano, A. Carbon nanotubes as free-radical scavengers. *J. Phys. Chem. C* **112**, 8922-8927 (2008).
49. Bartberger, M.D. et al. The reduction potential of nitric oxide (NO) and its importance to NO biochemistry. *Proc. Natl. Acad. Sci. U. S. A.,* **99**, 10958-10963 (2002).

**Figure 1.**

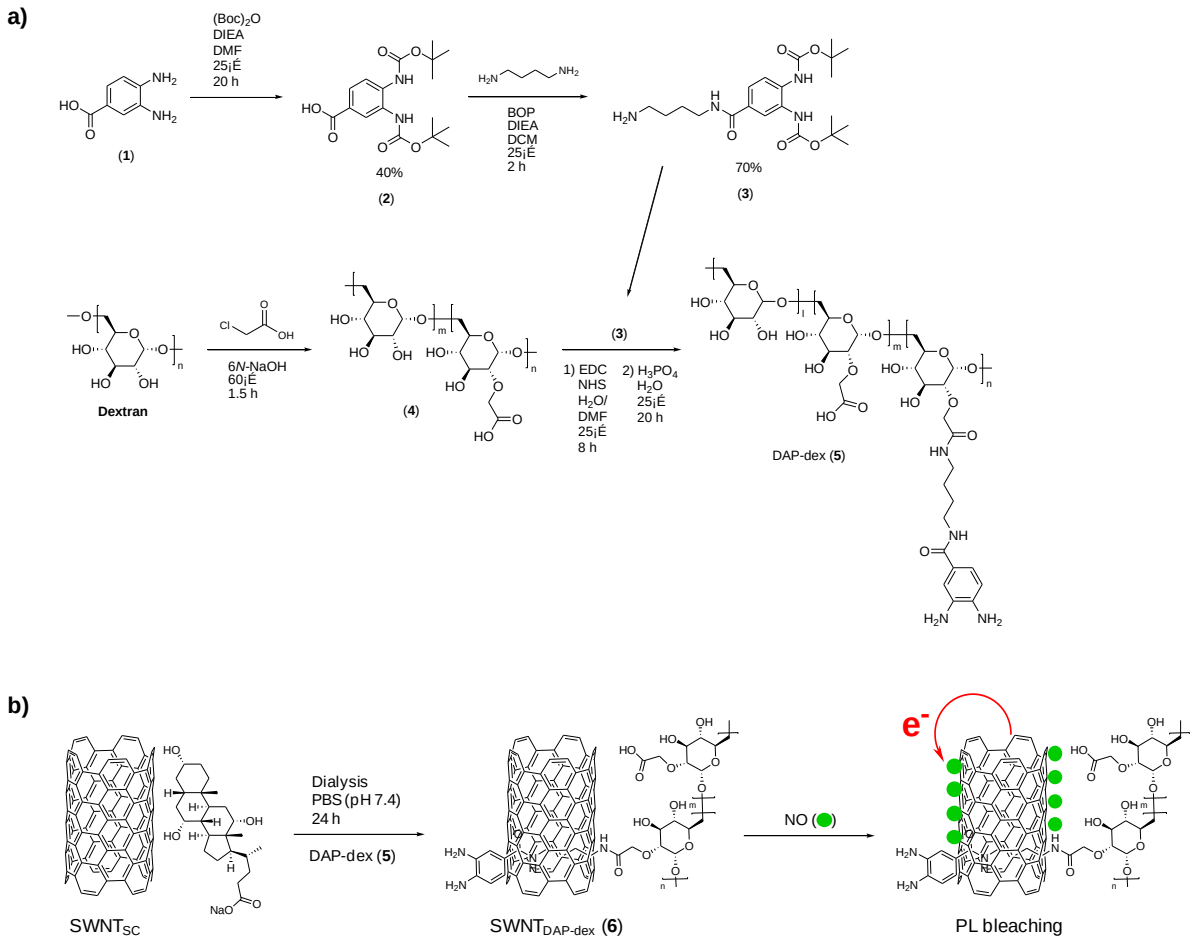
a)
(Boc)2O
DIEA
DMF
25¡É
20 h
(1)
40%
(2)
BOP
DIEA
DCM
25¡É
2 h
70%
(3)
Dextran
6N-NaOH
60¡É
1.5 h
(4)
(3)
1) EDC
NHS
H2O/
DMF
25¡É
8 h
2) H3PO4
H2O
25¡É
20 h
DAP-dex (5)
b)
SWNTSC
Dialysis
PBS (pH 7.4)
24 h
DAP-dex (5)
SWNTDAP-dex (6)
NO
e-
PL bleaching

**Figure 2.**

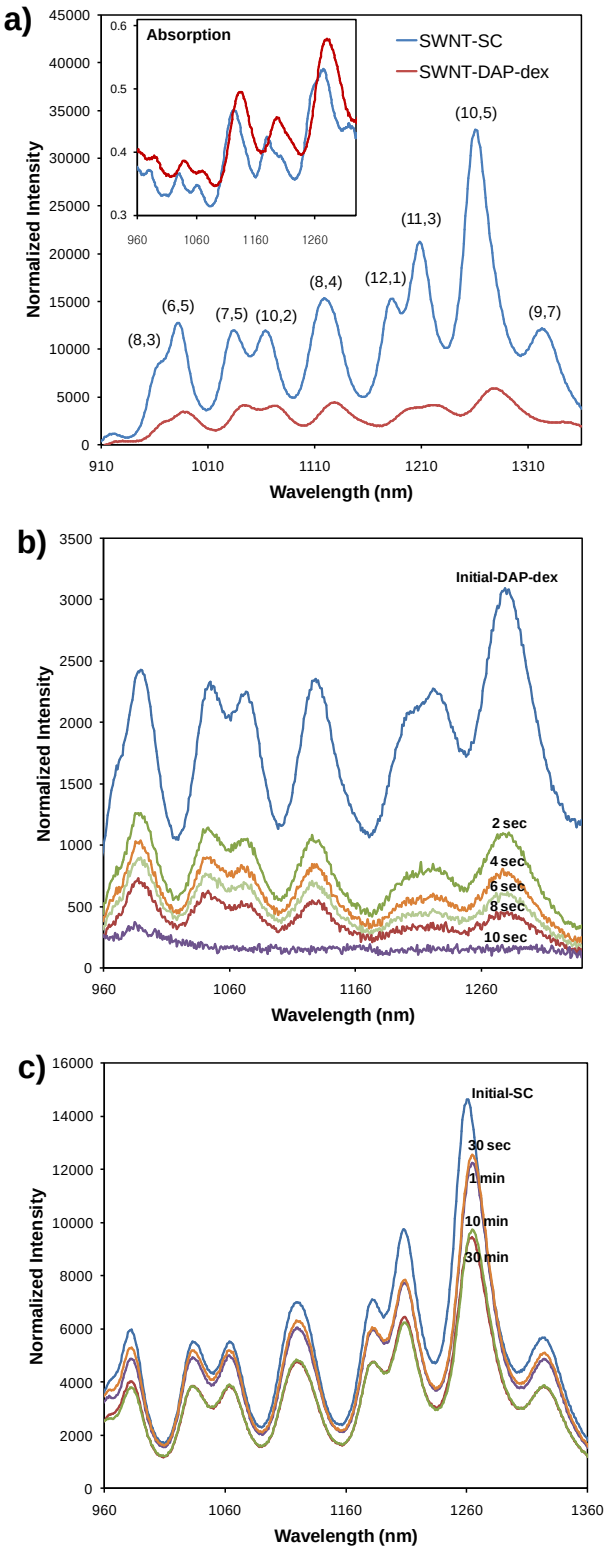
a)
Absorption
SWNT-SC
SWNT-DAP-dex
Normalized Intensity
Wavelength (nm)
(8,3)
(6,5)
(7,5)
(10,2)
(8,4)
(12,1)
(11,3)
(10,5)
(9,7)
b)
Initial-DAP-dex
2 sec
4 sec
6 sec
8 sec
10 sec
Normalized Intensity
Wavelength (nm)
c)
Initial-SC
30 sec
1 min
10 min
30 min
Normalized Intensity
Wavelength (nm)

**Figure 3.**

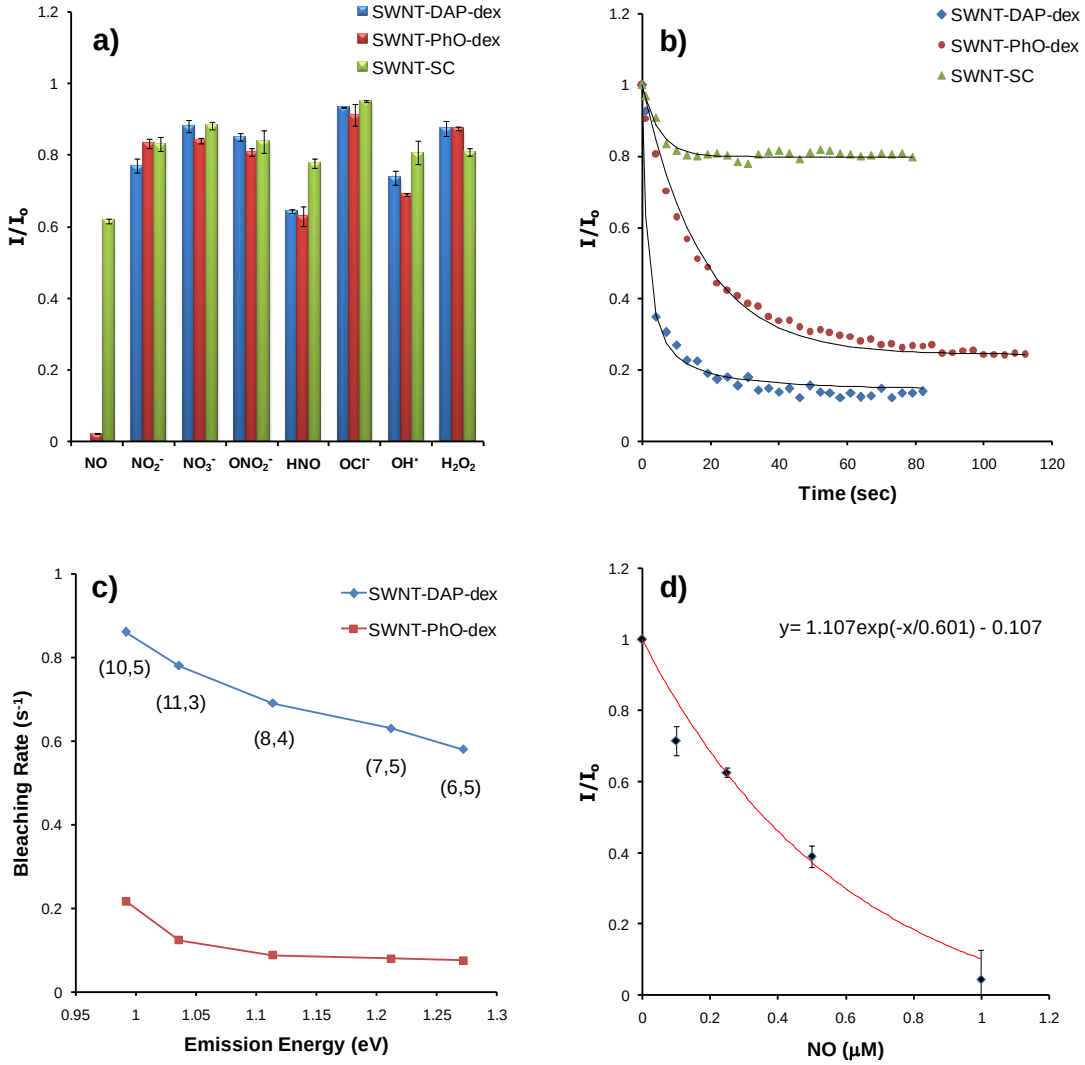
a)
SWNT-DAP-dex
SWNT-PhO-dex
SWNT-SC
I/I$_o$
NO
NO$_2^-$
NO$_3^-$
ONO$_2^-$
HNO
OCl$^-$
OH$^•$
H$_2$O$_2$
b)
SWNT-DAP-dex
SWNT-PhO-dex
SWNT-SC
I/I$_o$
Time (sec)
c)
SWNT-DAP-dex
SWNT-PhO-dex
(10,5)
(11,3)
(8,4)
(7,5)
(6,5)
Bleaching Rate (s$^{-1}$)
Emission Energy (eV)
d)
y= 1.107exp(-x/0.601) - 0.107
I/I$_o$
NO (μM)

**Figure 4.**

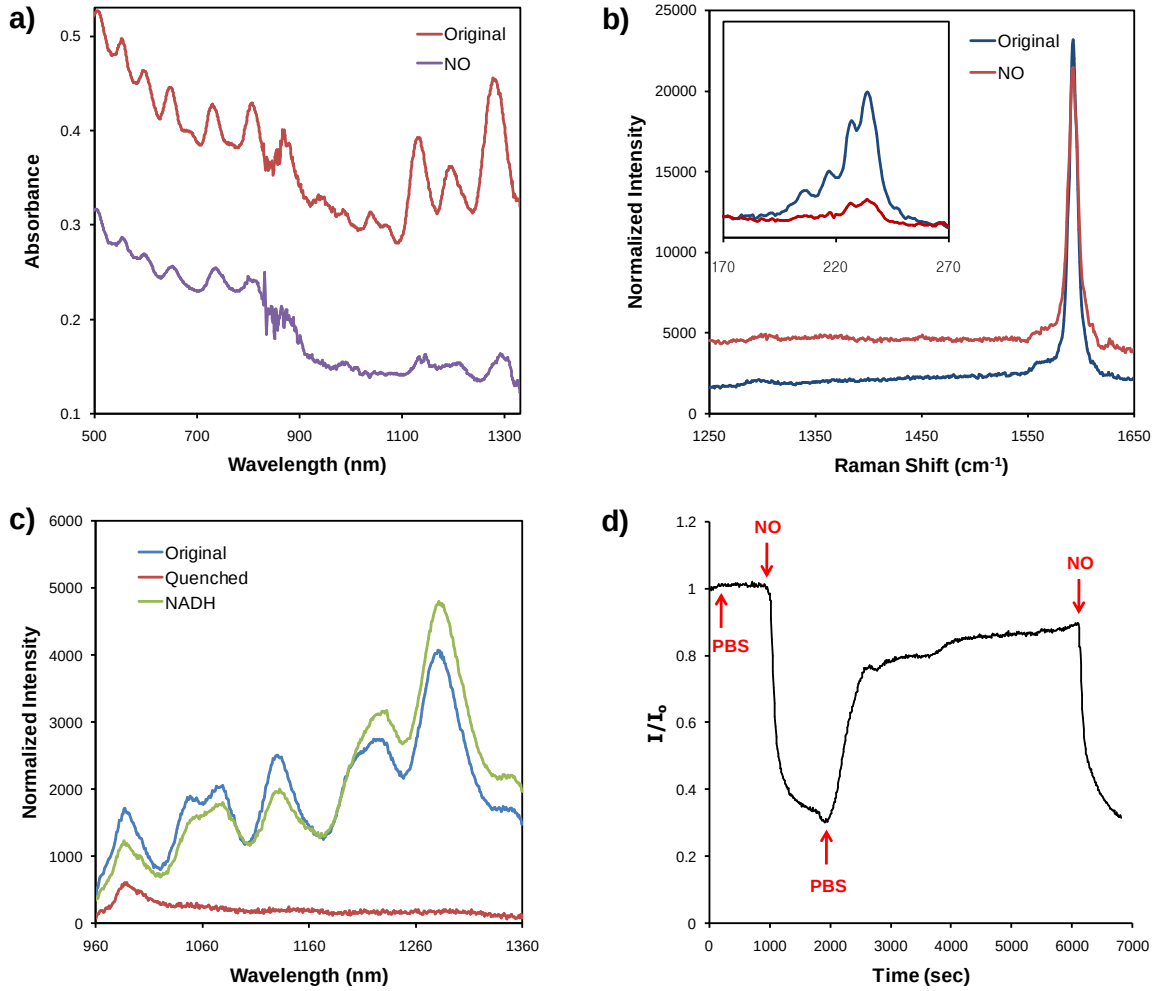
a)
Original
NO
Absorbance
Wavelength (nm)
b)
Original
NO
Normalized Intensity
Raman Shift (cm-1)
c)
Original
Quenched
NADH
Normalized Intensity
Wavelength (nm)
d)
NO
NO
PBS
PBS
I/I0
Time (sec)

**Figure 5.**

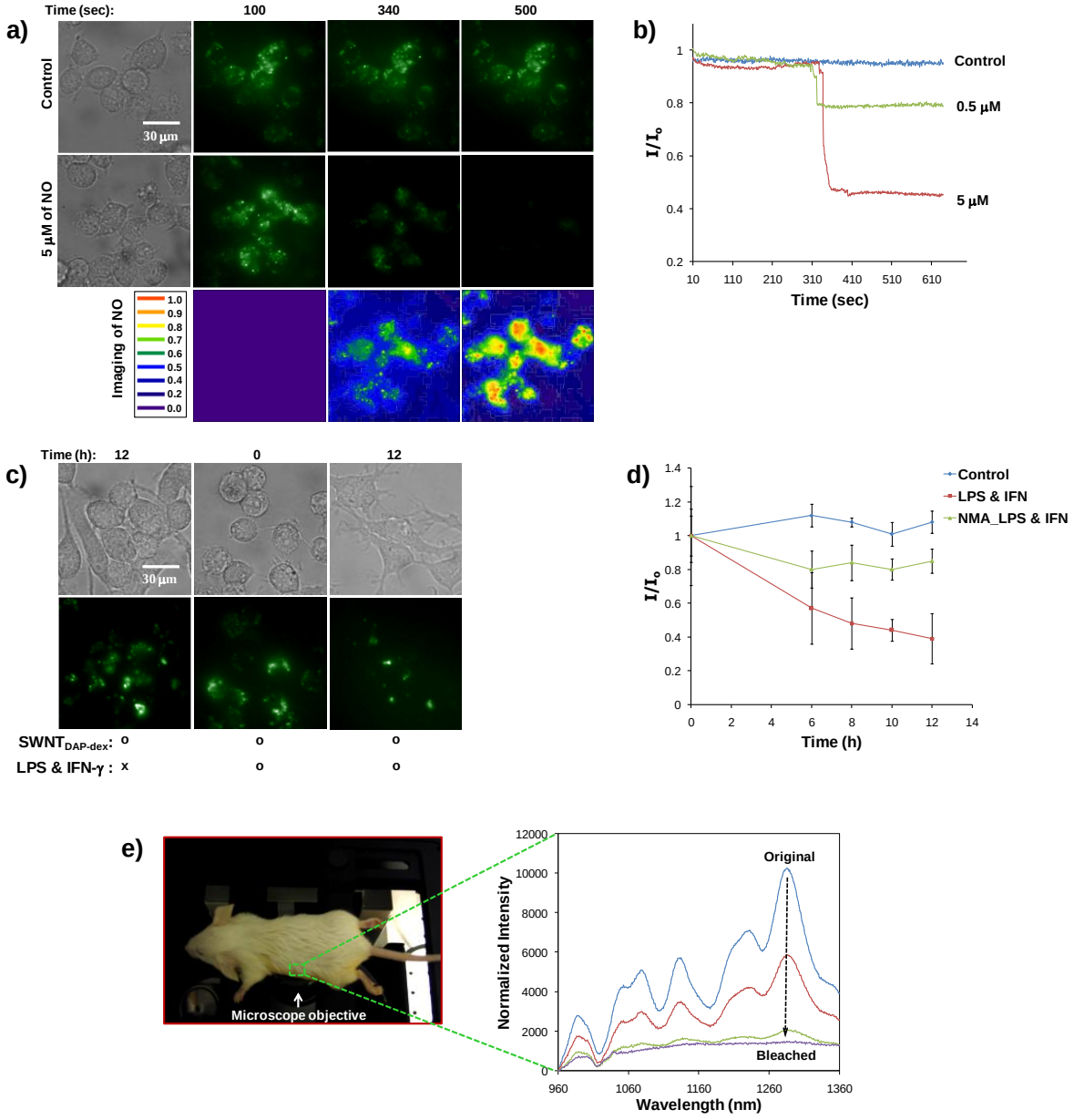
a)
Time (sec):
100
340
500
Control
5 μM of NO
Imaging of NO
30 μm
1.0
0.9
0.8
0.7
0.6
0.5
0.4
0.2
0.0
b)
Control
0.5 μM
5 μM
I/I$_o$
Time (sec)
c)
Time (h):
12
0
12
30 μm
SWNT$_{DAP-dex}$:
LPS & IFN-γ :
d)
Control
LPS & IFN
NMA_LPS & IFN
I/I$_o$
Time (h)
e)
Microscope objective
Original
Bleached
Normalized Intensity
Wavelength (nm)